RESEARCH MEMORANDUM

WIND-TUNNEL DATA ON THE LONGITUDINAL AND LATERAL-DIRECTIONAL ROTARY DERIVATIVES OF A STRAIGHT-WING, RESEARCH AIRPLANE CONFIGURATION AT MACH NUMBERS FROM 2.5 TO 3.5

By Benjamin H. Beam and Kenneth C. Endicott

Ames Aeronautical Laboratory
Moffett Field, Calif.

NATIONAL ADVISORY COMMITTEE
FOR AERONAUTICS
WASHINGTON
March 25, 1958

NACA RM A58A14

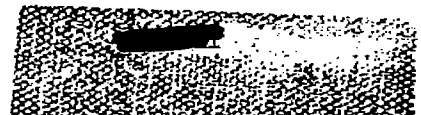

NATIONAL ADVISORY COMMITTEE FOR AERONAUTICS

RESEARCH MEMORANDUM

WIND-TUNNEL DATA ON THE LONGITUDINAL AND LATERAL-DIRECTIONAL ROTARY DERIVATIVES OF A STRAIGHT-WING, RESEARCH AIRPLANE CONFIGURATION AT MACH NUMBERS FROM 2.5 TO 3.5

By Benjamin H. Beam and Kenneth C. Endicott

SUMMARY

Results of wind-tunnel oscillation tests to measure the rotary derivatives of a research airplane configuration at supersonic speeds are presented. The wing of the model airplane was swept back 36.75° at the leading edge and had a taper ratio of 0.2 and an aspect ratio of 2.5. The area of the vertical tail was symmetrically disposed above and below the fuselage. Tests were conducted at Mach numbers of 2.5, 3.0, and 3.5 at a constant Reynolds number of 1,500,000 based on the wing mean aerodynamic chord and at angles of attack from -8° to +14°. Measurements were made of the damping in yaw, pitch, and roll, the static longitudinal and directional stability derivatives, the effective-dihedral derivative, the rolling moment due to yawing, and the yawing moment due to rolling. The measured derivatives are compared with estimated values based on the linearized theory of supersonic flow.

The configuration was found to be statically stable throughout the Mach number range, although its stability was becoming marginal at high angles of attack at a Mach number of 3.5. The damping in yaw and pitch were found to be higher than anticipated and it appeared that at the higher Mach numbers the damping contribution of the fuselage may be a very significant part of the total damping.

INTRODUCTION

An analysis of the dynamic motions of an airplane is of fundamental importance in modern airplane design. A necessary part of the calculation of representative airplane dynamics is a reasonably accurate knowledge of the stability derivatives. A number of theoretical reports have been

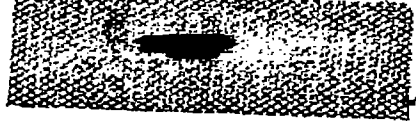

published which present first-order values of the rotary derivatives for various configurations based on the linearized theory of supersonic flow. References 1 and 2 are representative examples. The applicability of these methods depends to a large extent on the proper combination of the effects of the separate components of the airplane, such as the wing, the fuselage, and the tail surfaces, with due regard for the influence of one component on another. Although the proper combination of these effects has been the subject of research at lower Mach numbers, very little experimental data on the rotary derivatives exist for Mach numbers from 2.5 to 3.5. It is, therefore, of interest to compare values of the rotary derivatives obtained from conventional methods of estimation which have been found applicable at lower speeds with measured data at the higher supersonic Mach numbers.

This report presents experimental values of stability derivatives from wind-tunnel oscillation tests of a model of a research airplane configuration and comparisons with values estimated from theory for Mach numbers of 2.5, 3.0, and 3.5 at angles of attack from -8° to $+14^\circ$. Some additional data are presented for the basic configuration with the vertical tail surfaces removed to show the separate effects of the vertical tail. The derivatives are referred to a body system of axes and include the damping in pitch derivative $(C_{m_q} + C_{m_{\dot{\alpha}}})$, the static longitudinal stability derivative (C_{m_α}), the damping in roll derivative $(C_{l_p} + C_{l_{\dot{\beta}}} \sin \alpha)$, the rolling moment due to yawing derivative $(C_{l_r} - C_{l_{\dot{\beta}}} \cos \alpha)$, the rolling moment due to sideslip derivative (C_{l_β}), the damping in yaw derivative $(C_{n_r} - C_{n_{\dot{\beta}}} \cos \alpha)$, the yawing moment due to rolling derivative $(C_{n_p} + C_{n_{\dot{\beta}}} \sin \alpha)$, and the static directional stability derivative (C_{n_β}).

DEFINITIONS AND SYMBOLS

Forces, moments, and deflections are referred to a body system of axes defined in figure 1. The various stability derivatives are defined as follows:

C_{L_α} $\dfrac{\partial C_L}{\partial \alpha}$

C_{m_α} $\dfrac{\partial C_m}{\partial \alpha}$

$C_{m_{\dot{\alpha}}}$ $\dfrac{\partial C_m}{\partial (\dot{\alpha} \bar{c}_w / 2V)}$

C_{m_q} $\dfrac{\partial C_m}{\partial (q \bar{c}_w / 2V)}$

[redacted]

C_{Y_β} $\frac{\partial C_Y}{\partial \beta}$

C_{l_p} $\frac{\partial C_l}{\partial (pb/2V)}$

C_{l_r} $\frac{\partial C_l}{\partial (rb/2V)}$

C_{l_β} $\frac{\partial C_l}{\partial \beta}$

$C_{l_{\dot{\beta}}}$ $\frac{\partial C_l}{\partial (\dot{\beta}b/2V)}$

C_{n_p} $\frac{\partial C_n}{\partial (pb/2V)}$

C_{n_r} $\frac{\partial C_n}{\partial (rb/2V)}$

C_{n_β} $\frac{\partial C_n}{\partial \beta}$

$C_{n_{\dot{\beta}}}$ $\frac{\partial C_n}{\partial (\dot{\beta}b/2V)}$

The following additional symbols are used in the report:

A aspect ratio, $\frac{b^2}{S}$

B $\sqrt{M^2-1}$

b wing span

C_L lift coefficient, $\frac{\text{lift}}{\frac{1}{2}\rho V^2 S_W}$

C_l rolling-moment coefficient, $\frac{\text{rolling moment}}{\frac{1}{2}\rho V^2 S_W b}$

C_m pitching-moment coefficient, $\frac{\text{pitching moment}}{\frac{1}{2}\rho V^2 S_W \bar{c}_W}$

C_n yawing-moment coefficient, $\frac{\text{yawing moment}}{\frac{1}{2}\rho V^2 S_W b}$

C_Y side-force coefficient, $\frac{\text{side force}}{\frac{1}{2}\rho V^2 S_W}$

c local chord

$\bar{c}$ mean aerodynamic chord, $\frac{2}{S}\int_0^{b/2} c^2 dy$

c_{l_α} two-dimensional lift-curve slope

l chordwise distance of the center of lift of the tail behind the moment reference

M Mach number

p rolling velocity

Q body volume

q pitching velocity

r yawing velocity

S area

S_b base area of fuselage

V velocity

X_{cg} chordwise distance of the aerodynamic center of the wing behind the moment reference

X_b distance of the base of the fuselage behind the moment reference

y spanwise coordinate

$\bar{y}$ spanwise distance of the mean aerodynamic chord from the plane of symmetry, $\frac{2}{S}\int_0^{b/2} cy\, dy$

[redacted]

Z_V distance of the aerodynamic center of the vertical tail above the fuselage reference line

α angle of attack, radians except where noted

β angle of sideslip, radians except where noted

Γ angle of geometric dihedral, deg

δ_H horizontal-tail incidence angle, positive deflection indicated in figure 1

ϵ angle of downwash

ρ air density

σ angle of sidewash

η tail efficiency factor

Λ sweepback angle of leading edge

λ taper ratio of wing

Subscripts

F fuselage

H horizontal tail

V vertical tail

W wing

MODEL

The model used for this investigation was a 0.09-scale reproduction of an early configuration of the X-15 research airplane, and was supplied by North American Aviation, Inc. A three-view drawing of the model showing some of the important dimensions is presented in figure 2. More detailed dimensional characteristics are presented in table I. Two views of the model mounted on the oscillation apparatus in the wind tunnel are shown in the photograph, figure 3.

[redacted]

The horizontal stabilizer was adjustable in 10 increments of incidence angle from +5° to -25° as required to reduce the static pitching moments to an acceptable level as explained in the section on Tests. For some of the tests reported herein, the top and bottom vertical tails were removed and replaced with fairings set flush with the fuselage.

The requirements of high strength and light weight necessary in models used for this type of testing were met using plastic laminated glass cloth for the fuselage shell and magnesium for the aerodynamic surfaces. An inner sleeve which mated to the oscillation mechanism and to which the fuselage and aerodynamic surfaces were attached was also made of magnesium. The total weight of the model was 15 pounds.

APPARATUS

Tests were conducted in the 8- by 7-foot supersonic test section of the Ames Unitary Plan wind tunnel. This wind tunnel is capable of continuous variation of Mach number from 2.5 to 3.5 and of stagnation pressure from 2 to 28 pounds per square inch absolute. A more detailed description of the wind tunnel may be found in reference 3.

The oscillation test apparatus described in reference 4 was used for the tests reported herein. This apparatus consists of two dynamic balances with supplementary electronic equipment for establishing a steady-state forced oscillation of the model and for measuring the desired moments and deflections within the balance for evaluation of the stability derivatives. The model oscillation was of a single degree of freedom with an amplitude between ±1° and ±2°. One balance was used to measure the pitching and yawing derivatives. The other balance was used for the rolling derivatives. Deflection galvanometers indicated visually the steady-state values of oscillation amplitude, input torque required to maintain the oscillation, and, for the yaw tests, the rolling moment due to yawing velocity. The oscillation frequency varied from 4 to 8 cycles per second, depending on the natural oscillation frequency of the model on the crossed-flexure spring support within the balance, and was indicated visually on an electronic counter. Additional description of the details of the technique can be found in reference 4.

TESTS

Tests were made at Mach numbers of 2.5, 3.0, and 3.5 through a range of angles of attack from -8° to +14°. The Reynolds number for the tests was 1.5 million referred to the mean aerodynamic chord of the wing. The design of the oscillation apparatus was such that it was necessary to limit static pitching moments to approximately ±200 inch-pounds for the

damping in pitch tests, and ±800 inch-pounds for the lateral-directional derivative tests. The horizontal stabilizer on the model was used as a trimming device to maintain the static pitching moments within these limits. Three positions of the stabilizer were required for the damping in pitch tests to cover the range of angles of attack, but one position sufficed for the lateral-directional derivative tests.

ACCURACY AND CORRECTIONS TO DATA

Corrections to the measured values of the damping derivatives due to internal damping of the model and oscillation mechanism were determined from measurements of the damping at zero airspeed with the wind tunnel evacuated immediately prior to each set of test runs on a particular configuration. Application of these corrections changed the measured values of C_{l_p} and C_{n_r} by an increment of approximately 0.14, and $C_{m_q} + C_{m_{\dot{\alpha}}}$ by 1.0.

A source of random error in the data was introduced by the accuracy with which the indicated values could be read on the deflection galvanometers. Other errors were estimated to be negligible compared with the scatter in the galvanometer readings due to wind-tunnel turbulence and random aerodynamic effects. The random error in each of the eight measured stability derivatives is indicated by the scatter in the experimental data for the respective derivatives presented in the results.

RESULTS AND DISCUSSION

The results of this investigation are presented in figures 4 through 15. The calculated values of the stability derivatives, presented on the figures for comparison, are based on linearized supersonic flow theory taken from a number of sources. In adding together the contributions of the separate parts of the airplane, it has been necessary to make approximations which, in the absence of static-force data, cannot be critically examined. It has been assumed in calculating the theoretical values of the derivatives that the effective area of the lifting surface was that obtained by projecting the leading and trailing edges to the center of the fuselage. The change in downwash and sidewash at the tail due to the presence of the wing and fuselage was assumed to be zero for this configuration, and the dynamic pressure acting on the tail surfaces was assumed to be the free-stream value.

It is known, of course, that the above assumptions are not justified in many cases. However, the methods of correcting the theoretical values to account for these effects are not so clear. The most expeditious and

[redacted]

consistent manner of presenting the comparisons between theory and experiment appears to be through the use of the above assumptions. The particular equations used in calculating the derivatives are presented in the appendix, and can be modified to include the effects of assumptions different from those described above.

The Longitudinal Derivatives

Static longitudinal stability derivative, C_{m_α}.- It is apparent from figure 4 that the static longitudinal stability varied quite markedly with angle of attack. Although the basic configuration was statically stable in this range of Mach numbers, there was evidence of a decrease in stability at angles of attack from 8° to 10°. This would be expected to become more troublesome if the Mach number were increased since the stabilizing wing and tail contribution would decrease while the destabilizing fuselage contribution would remain relatively constant. Thus, increasing Mach number resulted in less negative values of C_{m_α} as illustrated in figure 6, and at an angle of attack of 10° C_{m_α} was becoming marginal at the higher Mach numbers.

The estimated values of C_{m_α} which have been placed in figure 4 are considerably more negative than those of the experimental data. It is neither surprising nor disturbing that this is so, however, as the lack of satisfactory purely theoretical methods of estimating C_{m_α} has resulted in great reliance on wind-tunnel static force data to obtain this derivative. If a smaller effective tail area (such as the exposed horizontal-tail area) had been used, or if a value of $d\epsilon/d\alpha$ of about 0.5 had been assumed, considerably better agreement with experiment would have been obtained at low angles of attack. Although some modification of the assumed values of tail area and downwash is indicated, it is also likely that the extended side fairings along the fuselage play an important role which has not been considered in the estimates. By use of the approximate methods of estimation indicated in the appendix, and in the absence of static force data to define more clearly the contributions of the separate components, the difference between theory and experiment indicated in figure 4 would seem to be representative of the accuracy to be expected in estimating C_{m_α} for this configuration.

Damping in pitch derivative, $C_{m_q} + C_{m_{\dot{\alpha}}}$.- The experimental values of damping in pitch derivative were negative (indicating stability) and varied little with angle of attack in the range at which tests were conducted (fig. 5). The variations in damping with horizontal stabilizer angle do not appear to be large and are within the experimental scatter. One surprising result is that the magnitude of the damping in pitch

derivative appeared to be increasing with Mach number at a Mach number of 3.5, whereas the theory indicates a reduction in magnitude with increasing Mach number.

Estimation of the effects of the horizontal tail on damping in pitch is subject to the same uncertainty as noted previously in connection with C_{m_α}. It is worthwhile to note that a reduction in effective tail area, which would have improved the agreement between theory and experiment in the case of C_{m_α} would result in poorer agreement in the case of $C_{m_q} + C_{m_{\dot{\alpha}}}$. The effect of wing downwash on the horizontal tail can be examined to some extent by considering the effect of variations in assumed values of $d\epsilon/d\alpha$ in computing both C_{m_α} and $C_{m_q} + C_{m_{\dot{\alpha}}}$. The assumption of a positive value of $d\epsilon/d\alpha$ at zero angle of attack would result in better agreement in both cases. In accounting for the decrease in C_{m_α} at the higher angles of attack (fig. 4), however, the assumption of an increasing $d\epsilon/d\alpha$ with increasing angle of attack is required. This assumption would result in similarly large increased values of $C_{m_q} + C_{m_{\dot{\alpha}}}$ at the higher angles of attack which is not borne out by the experimental data (fig. 5) at least for Mach numbers of 3.0 and 3.5. The fact that the damping in pitch did not decrease with increasing Mach number suggests that perhaps the effects of the fuselage or of the extended fuselage side fairings may be more important than estimates indicate. Some data supporting this latter view will be discussed later in connection with the damping in yaw characteristics.

The Sideslip Derivatives

Static directional stability derivative, C_{n_β}.- The measured values of C_{n_β} for the basic airplane configuration and for the vertical-tail-off configuration are presented in figure 7. The comparisons with estimated values show that at zero lift the directional stability of the airplane with the vertical tail removed can be estimated fairly accurately. One noteworthy point with respect to the vertical-tail-off data is that at the higher angles of attack the directional stability improved with increasing Mach number. For example, at a Mach number of 2.5 C_{n_β} with the tail off became progressively more negative with increasing angle of attack, but at a Mach number of 3.5 C_{n_β} with the tail off was more nearly constant with angle of attack.

The tail contribution, obtained as the difference in C_{n_β} between the basic configuration and the vertical-tail-off configuration, was about 80 percent of the estimated tail contribution at zero angle of attack. The measured tail contribution, evaluated as the difference

[redacted]

between the basic and tail-off configurations, was approximately constant with variations in angle of attack for Mach numbers of 2.5 and 3.0. At a Mach number of 3.5, however, the tail contribution at the higher angles of attack was reduced, presumably because of interference from the fuselage and wing flow field on the upper vertical tail (ref. 5).

The variation of C_{n_β} for the basic configuration with Mach number and angle of attack was such that at 10° angle of attack the static directional stability was becoming marginal for Mach numbers greater than 3.5 (fig. 9). In fact, if the trend shown in figure 9 for 10° angle of attack were continued at the higher Mach numbers, the directional stability would have become zero at a Mach number of approximately 4.

Effective dihedral derivative, C_{l_β}.- At zero angle of attack C_{l_β} for the basic configuration was positive at all Mach numbers as shown in figure 8. In the estimations this is accounted for solely by the effect of negative geometric dihedral in the horizontal tail. The wing had no geometric dihedral and the vertical-tail area was symmetrically disposed above and below the fuselage reference axis. The contribution of the wing to C_{l_β} was determined to be negligible on the basis of separate calculations for the effect of leading-edge sweep, tip effect, and trailing-edge sweep as indicated in the appendix. On the basis of these simplified calculations, C_{l_β} for the vertical-tail-off configuration should not have varied with angle of attack. In figure 8 it is shown that C_{l_β} became more negative with increasing angle of attack for the vertical-tail-off configuration, and this may have been due to interference from the fuselage and a resultant loss of lift on the trailing wing during sideslip. The reason for the change in vertical-tail contribution to C_{l_β} with angle of attack was probably a reduction in effectiveness of the upper vertical tail at positive angles of attack, and the lower vertical tail at negative angles of attack.

The Yawing Derivatives

Damping in yaw derivatives, $C_{n_r} - C_{n_{\dot\beta}}\cos\alpha$.- The damping in yaw is seen from figure 10 to have been stabilizing (negative value of the derivative) and approximately constant with angle of attack in the range of Mach numbers at which tests were conducted. The comparison between the estimated and measured values of $C_{n_r} - C_{n_{\dot\beta}}\cos\alpha$ is also of considerable interest. The agreement between the estimated and measured values for the basic configuration is fairly good. However, the estimated relative contributions of the vertical tail and the wing-body horizontal tail are considerably different from the incremental values obtained from the experimental results.

[redacted]

The estimated values of the tail contribution can be made to agree more nearly with the experimental results if a smaller effective tail area is assumed. A comparison of the data in figure 10 with that in figure 7 indicates that in the estimation of both the static directional stability and the damping in yaw, the tail has been assumed to be more effective than the experimental data would indicate. The assumption that only the exposed tail area was effective in producing damping in yaw would reduce the tail contribution to about 60 percent of the estimated values indicated in figure 10, and would then agree fairly well with the experimental values of tail contribution.

No such explanation is possible in the case of the data for the vertical-tail-off configuration shown in figure 10. Since the contribution of the wing and horizontal tail can be assumed negligible, the estimated values shown are for the body alone, the side fairings along the fuselage being neglected. It appears that the damping of the vertical-tail-off configuration was 2-1/2 to 3 times the estimated value and comprised over 60 percent of the total damping in yaw at a Mach number of 3.5. This contribution varied only slightly with Mach number, increasing with increasing Mach number in the range over which tests were conducted (fig. 12).

Rolling moment due to yawing derivative, $C_{l_r} - C_{l_\beta} \cos \alpha$.- The rolling moment due to yawing is shown in figure 11 to have been nearly zero for all Mach numbers within the accuracy of experimental measurement. Theory indicates a slightly negative value of this derivative due to cathedral in the horizontal tail.

The Rolling Derivatives

Damping in roll derivative, $C_{l_p} + C_{l_\beta} \sin \alpha$.- The damping in roll of this configuration was stable (negative values of the derivative) at all Mach numbers and angles of attack within the range over which tests were conducted (fig. 13). Estimated values from reference 6 agree well with the experimental data for most conditions. The reason for the differences shown between theory and experiment at a Mach number of 3 and for angles of attack above 8° is not known; the same trend is not apparent in the data for Mach numbers of 2.5 and 3.5. The data confirm the expected slight decrease in damping in roll with increasing Mach number in the range over which tests were conducted (fig. 15).

Yawing moment due to rolling derivative, $C_{n_p} + C_{n_\beta} \sin \alpha$.- Values of $C_{n_p} + C_{n_\beta} \sin \alpha$ obtained experimentally were found to be predominantly negative (fig. 14). Theory indicates a slightly negative value of this

derivative due to the cathedral in the horizontal tail. The experimental scatter, indicated in the data of figure 14, is greater than the differences between theory and experiment.

SUMMARY OF RESULTS

Results of wind-tunnel oscillation tests on a model of a straight-wing, research airplane configuration in a range of Mach numbers from 2.5 to 3.5 indicate the following:

1. The model was statically stable longitudinally and directionally through the range of Mach numbers at which tests were conducted. However, both longitudinal and directional stability were becoming marginal with increasing Mach number at an angle of attack of 10° and a Mach number of 3.5.

2. The rolling moment due to sideslip was slightly positive at zero angle of attack but became negative at angles of attack from 6° to 10°.

3. The measured values of damping in pitch were somewhat higher than values estimated by methods applicable at lower Mach numbers.

4. Measured values of damping in yaw were higher than estimated. The damping in yaw with the vertical tail removed was approximately three times the estimated value, and was a very significant part of the total damping, particularly at the higher Mach numbers.

5. The damping in roll, yawing moment due to rolling, and rolling moment due to yawing were in agreement with estimated values within the accuracy of measurement.

Ames Aeronautical Laboratory
National Advisory Committee for Aeronautics
Moffett Field, Calif., Jan. 14, 1958

[redacted]

APPENDIX

STABILITY DERIVATIVE ESTIMATES

The equations used and the assumptions made to obtain the calculated values of the stability derivatives shown in figures 4 through 15 are summarized below. All calculations were made for the body system of axes defined in figure 1. In the following equations it is assumed that the separate effects of the fuselage, wing, horizontal tail, and vertical tail can be superimposed. Where possible, references have been included for the specific equations which more completely define or justify the applicability of the equations.

Static Longitudinal Stability Derivative, C_{m_α}

$$C_{m_\alpha} = \left(C_{m_\alpha}\right)_F + \left(C_{m_\alpha}\right)_W + \left(C_{m_\alpha}\right)_H \tag{1}$$

$$\left(C_{m_\alpha}\right)_F = 2\left(\frac{Q - S_b X_b}{S_W \bar{c}_W}\right) \quad \text{(ref. 7)} \tag{2}$$

The above equation neglects the effects of the side fairings along the fuselage, and viscous crossflow at angle of attack.

$$\left(C_{m_\alpha}\right)_W = -C_{L_\alpha}\frac{X_{cg}}{\bar{c}_W} = -\frac{4}{B}\left(1 - \frac{1}{2BA}\right)\frac{X_{cg}}{\bar{c}_W} \tag{3}$$

In equation (3) it is assumed that the lift of the wing is that given by the linear theory (refs. 8 and 9), and that the lift acts at the mid-point of the wing mean aerodynamic chord.

$$\left(C_{m_\alpha}\right)_H = -\frac{l_H}{\bar{c}_W}\left(C_{L_\alpha}\right)_H \eta_H \left(1 - \frac{d\epsilon}{d\alpha}\right) = -\frac{l_H}{\bar{c}_W}\frac{S_H}{S_W}\frac{4}{B}\left(1 - \frac{1}{2BA}\right) \tag{4}$$

In equation (4) the same assumptions are made as in equation (3). In addition, it is assumed that $d\epsilon/d\alpha = 0$ behind the wing (ref. 9), even though a part of the induced downwash inside the wing tip Mach cone impinges on the horizontal tail; η_H has been assumed equal to 1.

[redacted]

Damping in Pitch Derivative, $C_{m_q} + C_{m_{\dot{\alpha}}}$

$$C_{m_q} + C_{m_{\dot{\alpha}}} = \left(C_{m_q} + C_{m_{\dot{\alpha}}}\right)_F + \left(C_{m_q} + C_{m_{\dot{\alpha}}}\right)_W + \left(C_{m_q} + C_{m_{\dot{\alpha}}}\right)_H \tag{5}$$

$$\left(C_{m_q} + C_{m_{\dot{\alpha}}}\right)_F = -\frac{4S_b X_b^2}{S_W \bar{c}_W^2} \quad \text{(refs. 10 and 11)} \tag{6}$$

In equation (6) the effects of the extended fuselage side fairings are neglected as in equation (2).

$$\left(C_{m_q} + C_{m_{\dot{\alpha}}}\right)_W = -\frac{2}{3B} + \frac{1}{3B^3}\left(2 - \frac{2+B^2}{AB}\right) - \frac{1}{B^3}\left(\frac{8+4B^2}{3AB} - 4\right)\left(\frac{X_{cg}}{\bar{c}_W}\right) - \frac{8}{B}\left(1 - \frac{1}{2BA}\right)\left(\frac{X_{cg}}{\bar{c}_W}\right)^2 \quad \text{(ref. 2)} \tag{7}$$

$$\approx 0$$

In equation (7) it is assumed that the damping in pitch of the wing is that given by the linear theory for a rectangular wing having the same aspect ratio.

$$\left(C_{m_q} + C_{m_{\dot{\alpha}}}\right)_H = -2\left(\frac{l_H}{\bar{c}_W}\right)^2 \left(C_{L_\alpha}\right)_H \eta_H \left(1 + \frac{d\epsilon}{d\alpha}\right) \quad \text{(ref. 12, pp. 393-394)} \tag{8}$$

$$= -2\left(\frac{l_H}{\bar{c}_W}\right)^2 \frac{S_H}{S_W} \frac{4}{B}\left(1 - \frac{1}{2BA}\right)$$

which employs the same assumptions as in equation (4).

Static Directional Stability Derivative, C_{n_β}

$$C_{n_\beta} = \left(C_{n_\beta}\right)_F + \left(C_{n_\beta}\right)_V \tag{9}$$

where

$$\left(C_{n_\beta}\right)_F = -2\left(\frac{Q - S_b X_b}{S_W b}\right)$$

as in equation (2).

[redacted]

$$\left(C_{n_\beta}\right)_V = -\frac{l_V}{b}\left(C_{Y_\beta}\right)_V \eta_V \left(1 + \frac{d\sigma}{d\beta}\right) \qquad \text{(ref. 12, p. 324)} \qquad (10)$$

$$= \frac{l_V}{b}\frac{S_V}{S_W}\frac{4}{B}\left(1 - \frac{1}{2BA}\right)$$

The assumptions employed in equation (10) are similar to those in equation (4).

Effective Dihedral Derivative, C_{l_β}

$$C_{l_\beta} = \left(C_{l_\beta}\right)_W + \left(C_{l_\beta}\right)_H + \left(C_{l_\beta}\right)_V \qquad (11)$$

$\left(C_{l_\beta}\right)_W \approx 0$ from an analysis of the results of calculations made for related plan forms (refs. 1 and 2), although the hexagonal plan form of the wing of this report is not specifically considered

$$\left(C_{l_\beta}\right)_H = -\left(c_{l_\alpha}\right)_H \left(\frac{\bar{y}_H}{b}\right)\left(\frac{S_H}{S_W}\right) \sin \Gamma_H \qquad (12)$$

Equation (12) was obtained from a spanwise integration of the rolling moments induced by sideslip on the horizontal tail. With the assumption that $\left(c_{l_\alpha}\right)_H = 4/B$

$$\left(C_{l_\beta}\right)_H = -\frac{4}{B}\left(\frac{\bar{y}_H}{b}\right)\left(\frac{S_H}{S_W}\right) \sin \Gamma_H$$

$$\left(C_{l_\beta}\right)_V = \frac{Z_V}{b}\left(C_{Y_\beta}\right)_V \eta_V \left(1 + \frac{d\sigma}{d\beta}\right) \qquad (13)$$

$$= -\frac{Z_V}{b}\frac{S_V}{S_W}\frac{4}{B}\left(1 - \frac{1}{2BA}\right) = 0$$

since $Z_V = 0$. Equation (13) follows from equation (10).

Damping in Yaw Derivative, $C_{n_r} - C_{n_{\dot\beta}}\cos\alpha$

$$C_{n_r} - C_{n_{\dot\beta}}\cos\alpha = \left(C_{n_r} - C_{n_{\dot\beta}}\right)_F + \left(C_{n_r} - C_{n_{\dot\beta}}\right)_V \qquad (14)$$

[redacted]

Equation (14) follows from equation (5) by assuming small α for which $\cos \alpha \approx 1$. The contribution of the wing was calculated to be negligible (refs. 1 and 2).

$$\left(C_{n_r} - C_{n_{\dot{\beta}}}\right)_F = -\frac{4S_b x_b^2}{S_W b^2} \qquad \text{(from eq. (6))} \tag{15}$$

$$\left(C_{n_r} - C_{n_{\dot{\beta}}}\right)_V = 2\left(\frac{l_V}{b}\right)^2 \left(C_{Y_\beta}\right)_V \eta_V \left(1 - \frac{d\sigma}{d\beta}\right) \tag{16}$$

$$= -2\left(\frac{l_V}{b}\right)^2 \frac{S_V}{S_W} \frac{4}{B}\left(1 - \frac{1}{2BA}\right)$$

The assumptions in equation (16) are the same as those in equation (10), and the derivation follows that of equation (8).

Rolling Moment Due to Yawing Derivative, $C_{l_r} - C_{l_{\dot{\beta}}} \cos \alpha$

$$C_{l_r} - C_{l_{\dot{\beta}}} \cos \alpha = \left(C_{l_r} - C_{l_{\dot{\beta}}}\right)_W + \left(C_{l_r} - C_{l_{\dot{\beta}}}\right)_V + \left(C_{l_r} - C_{l_{\dot{\beta}}}\right)_H \tag{17}$$

$$\left(C_{l_r} - C_{l_{\dot{\beta}}}\right)_W \approx \left(C_{l_r}\right)_W \approx 0 \qquad \text{(refs. 1 and 2)} \tag{18}$$

$$\left(C_{l_r} - C_{l_{\dot{\beta}}}\right)_V = -2\left(\frac{l_V}{b}\right)\left(\frac{Z_V}{b}\right)\left(C_{Y_\beta}\right)_V \eta_V \left(1 - \frac{d\sigma}{d\beta}\right) \tag{19}$$

$$= 0$$

since $Z_V = 0$. Equation (19) follows from equation (16).

$$\left(C_{l_r} - C_{l_{\dot{\beta}}}\right)_H \approx \left(C_{l_r}\right)_H = 2\left(c_{l_\alpha}\right)_H \left(\frac{l_H}{b}\right)\left(\frac{\bar{y}_H}{b}\right)\left(\frac{S_H}{S_W}\right) \sin \Gamma_H \tag{20}$$

Equation (20) was obtained from a spanwise integration of the rolling moments induced by yawing velocity on chordwise strip elements of the horizontal tail. With the assumption that $\left(c_{l_\alpha}\right)_H = 4/B$, equation (20) becomes

$$\left(C_{l_r} - C_{l_{\dot{\beta}}}\right)_H \approx \frac{8}{B}\left(\frac{l_H}{b}\right)\left(\frac{\bar{y}_H}{b}\right)\left(\frac{S_H}{S_W}\right) \sin \Gamma_H$$

Damping in Roll Derivative, $C_{l_p} + C_{l_{\dot{\beta}}} \sin \alpha$

$$C_{l_p} + C_{l_{\dot{\beta}}} \sin \alpha = \left(C_{l_p}\right)_W + \left(C_{l_p}\right)_H + \left(C_{l_p}\right)_V \tag{21}$$

$$\left(C_{l_p}\right)_W = C_{l_p}(B, A_W, \Lambda_W, \lambda_W) \tag{22}$$

where $C_{l_p}(B, A_W, \Lambda_W, \lambda_W)$ is obtained from the formulas or charts of reference 6 for the appropriate Mach number, aspect ratio, leading-edge sweep, and taper ratio.

$$\left(C_{l_p}\right)_H = \frac{S_H}{S_W}\left(\frac{b_H}{b}\right)^2 C_{l_p}(B, A_H, \Lambda_H, \lambda_H) \tag{23}$$

$$\left(C_{l_p}\right)_V = \frac{S_V}{S_W}\left(\frac{b_V}{b}\right)^2 C_{l_p}(B, A_V, \Lambda_V, \lambda_V) \tag{24}$$

Yawing Moment Due to Rolling Derivative, $C_{n_p} + C_{n_{\dot{\beta}}} \sin \alpha$

$$C_{n_p} + C_{n_{\dot{\beta}}} \sin \alpha = \left(C_{n_p}\right)_W + \left(C_{n_p}\right)_V + \left(C_{n_p}\right)_H \tag{25}$$

Equation (24) employs the same assumptions as equation (21).

$$\left(C_{n_p}\right)_W \approx 0 \qquad \text{(refs. 1 and 2)} \tag{26}$$

$$\left(C_{n_p}\right)_V = -2\left(\frac{l_V}{b}\right)\left(\frac{Z_V}{b}\right)\left(C_{Y_\beta}\right)_V \qquad \text{(ref. 13)} \tag{27}$$

$$= 0$$

since $Z_V = 0$.

$$\left(C_{n_p}\right)_H = 2\left(c_{l_\alpha}\right)_H \left(\frac{l_H}{b}\right)\left(\frac{\bar{y}_H}{b}\right)\left(\frac{S_H}{S_W}\right) \sin \Gamma_H \tag{28}$$

Equation (28) is obtained from a spanwise integration of the yawing moments induced by rolling velocity on chordwise strip elements of the horizontal tail. With the assumption that $(c_{l_\alpha})_H = 4/B$,

$$\left(C_{n_p}\right)_H = \frac{8}{B}\left(\frac{l_H}{b}\right)\left(\frac{\bar{y}_H}{b}\right)\left(\frac{S_H}{S_W}\right)\sin \Gamma_H$$

REFERENCES

1. Jones, Arthur L., and Alksne, Alberta: A Summary of Lateral-Stability Derivatives Calculated for Wing Plan Forms in Supersonic Flow. NACA Rep. 1052, 1951.

2. Harmon, Sidney M.: Stability Derivatives at Supersonic Speeds of Thin Rectangular Wings With Diagonals Ahead of Tip Mach Lines. NACA Rep. 925, 1949. (Supersedes NACA TN 1706)

3. Huntsberger, Ralph F., and Parsons, John F.: The Design of Large High-Speed Wind Tunnels. Rep. AG 15/P6, AGARD, May 4, 1954, pp. 127-152.

4. Beam, Benjamin H.: A Wind-Tunnel Test Technique for Measuring the Dynamic Rotary Stability Derivatives at Subsonic and Supersonic Speeds. NACA Rep. 1258, 1956. (Supersedes NACA TN 3347)

5. Spearman, M. LeRoy, and Henderson, Arthur, Jr.: Some Effects of Aircraft Configuration on Static Longitudinal and Directional Stability Characteristics at Supersonic Mach Numbers Below 3. NACA RM L55L15a, 1956.

6. Harmon, Sidney M., and Jeffreys, Isabella: Theoretical Lift and Damping in Roll of Thin Wings With Arbitrary Sweep and Taper at Supersonic Speeds. NACA TN 2114, 1950.

7. Allen, H. Julian, and Perkins, Edward W.: A Study of Effects of Viscosity on Flow Over Slender Inclined Bodies of Revolution. NACA Rep. 1048, 1951. (Supersedes NACA TN 2044)

8. Vincenti, Walter G.: Comparison Between Theory and Experiment for Wings at Supersonic Speeds. NACA Rep. 1033, 1951. (Supersedes NACA TN 2100)

9. Hilton, W. F.: High-Speed Aerodynamics. Longmans, Green and Co., New York, 1951, pp. 300-303.

10. Tobak, Murray, Reese, David E., Jr., and Beam, Benjamin H.: Experimental Damping in Pitch of 45° Triangular Wings. NACA RM A50J26, 1950.

11. Dorrance, William H.: Nonsteady Supersonic Flow About Pointed Bodies of Revolution. Jour. Aero. Sci., vol. 18, no. 8, Aug. 1951, pp. 505-511.

12. Perkins, Courtland D., and Hage, Robert E.: Airplane Performance Stability and Control. John Wiley and Sons, Inc., New York, 1949.

[redacted]

13. Campbell, John P., and McKinney, Marion O.: Summary of Methods for Calculating Dynamic Lateral Stability and Response and for Estimating Lateral Stability Derivatives. NACA Rep. 1098, 1952. (Supersedes NACA TN 2409)

[redacted]

TABLE I.- GEOMETRIC CHARACTERISTICS OF MODEL

	Exposed	Total
Wing (chord plane on body center line)		
Aspect ratio, A_W	2.150	2.500
Taper ratio, λ_W	0.271	0.200
Leading-edge sweep angle, Λ_W, deg		36.75
Dihedral angle, deg		0
Incidence angle, deg		0
Twist, deg		0
Airfoil section	NACA 66005 (modified) 1-percent blunt trailing edge	
Thickness ratio, percent		5
Area, S_W, sq ft	0.851	1.620
Span, b_W, ft	1.352	2.01
Mean aerodynamic chord, ft	0.698	0.924
Horizontal tail		
Aspect ratio, A_H	2.39	2.92
Taper ratio, λ_H	0.299	0.206
Leading-edge sweep angle, Λ_H, deg		50.58
Dihedral angle, deg		-15°
Incidence angle, δ_H, deg	-45 to +15	
Twist, deg		0
Airfoil section	NACA 66005 (modified) 1-percent blunt trailing edge	
Thickness ratio, percent		5
Area, S_H, sq ft	0.403	0.898
Span, b_H, ft	0.982	1.620
Mean aerodynamic chord, $\bar{c}_H$, ft	0.444	0.635
Length (0.25 $\bar{c}_W$ to 0.50 $\bar{c}_H$), l_H, ft	1.398	1.234
Spanwise location of $\bar{c}_H$ (from plane of symmetry), $\bar{y}$, ft		0.318
Height ($\bar{c}_H$ below wing chord plane)	-0.028	-0.030
Vertical tail (symmetrical about wing chord plane)		
Aspect ratio, A_V	1.11	1.298
Taper ratio, λ_V	0.778	0.696
Leading-edge sweep angle, deg		28.9
Airfoil section	11.5° double wedge	
Thickness ratio, percent		11.1
Area, S_V	0.647	1.069
Span, b_V	0.844	1.178
Mean aerodynamic chord, ft	0.857	0.915
Length (0.25 $\bar{c}_W$ to 0.50 $\bar{c}_V$), l_V, ft	1.20	1.23

[redacted]

TABLE I.- GEOMETRIC CHARACTERISTICS OF MODEL - Concluded

	Extended fuselage side fairings not included	Extended fuselage side fairings included
Fuselage		
Fineness ratio	10.5	9.4
Length, ft	4.425	4.425
Volume, cu ft	0.525	0.625
Base area, sq ft	0.101	0.161
Frontal area	0.139	0.173
Moment reference (on body center line)		
Longitudinal location		
Aft of leading edge of $\bar{c}$		$0.25\bar{c}$
Aft of nose, ft		2.618

[redacted]

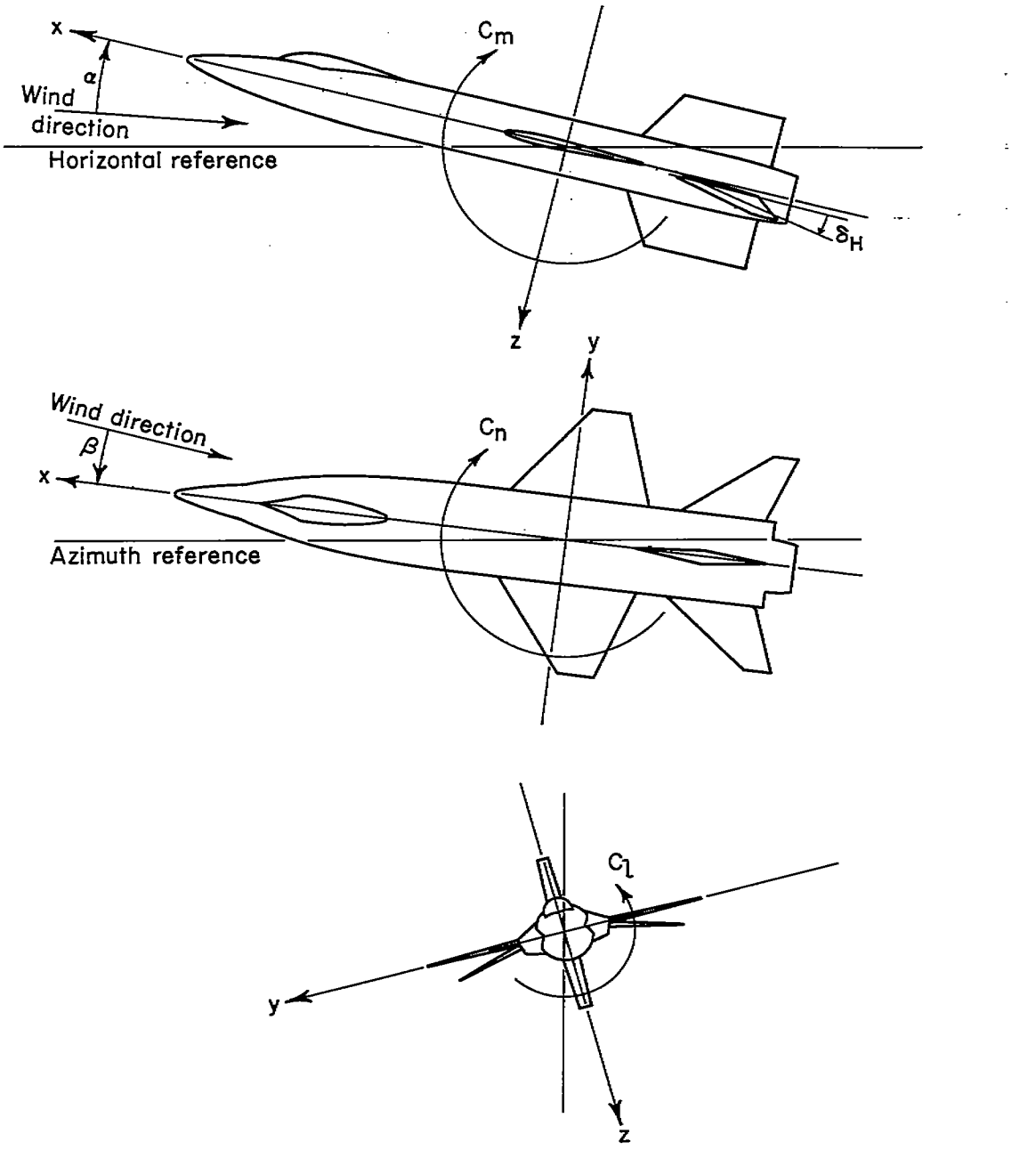

Figure 1.- The body system of axes. Arrows indicate positive directions of moments, forces, and angles. This system of axes is defined as an orthogonal system having the origin at the moment reference point and in which the x axis is parallel to the longitudinal axis of the body, the z axis is in the plane of symmetry and perpendicular to the x axis, and the y axis is perpendicular to the plane of symmetry.

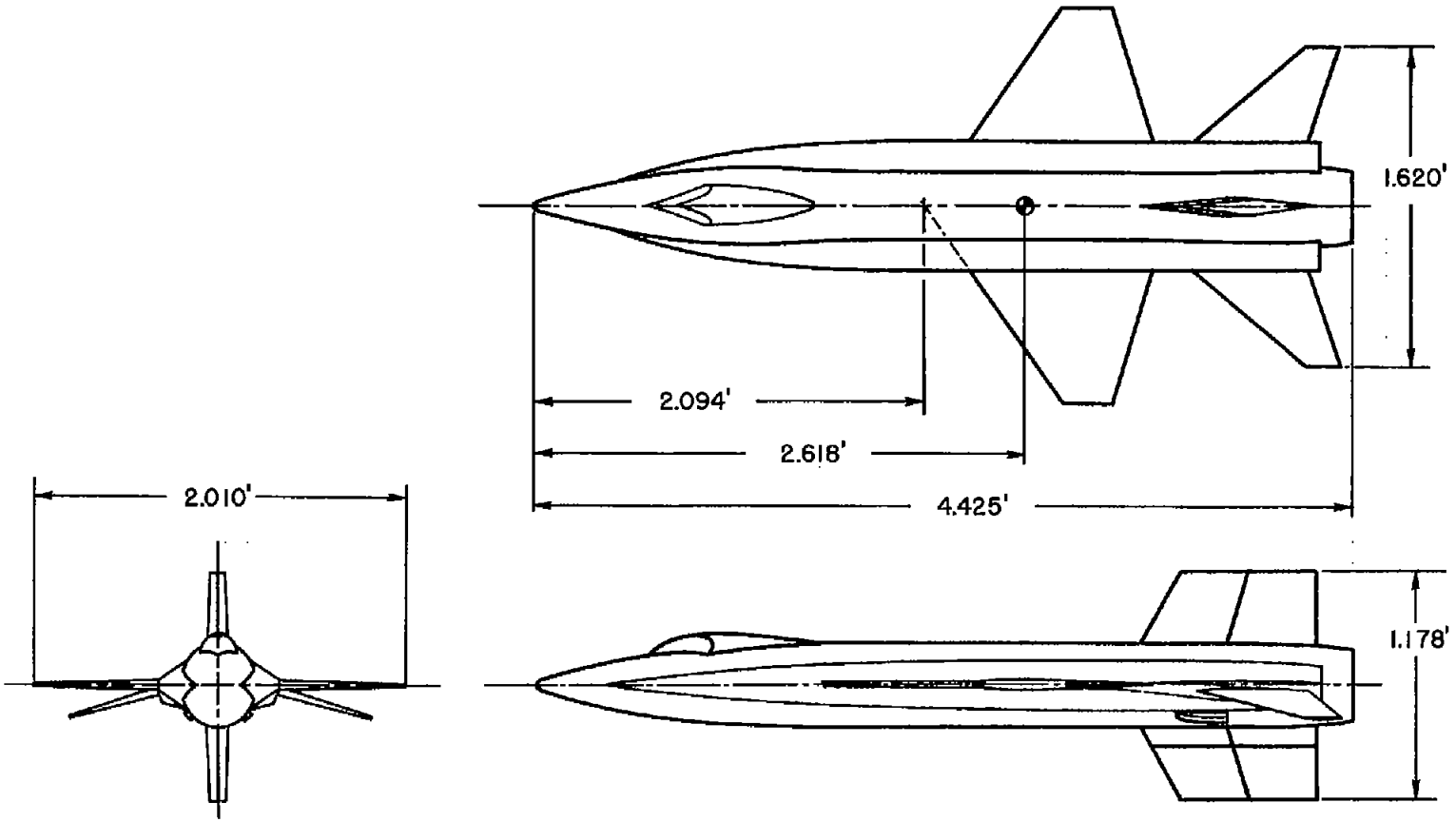

Figure 2.- Sketch of the airplane model showing some of the important dimensions.

A-22162

(a) Front-quarter view.

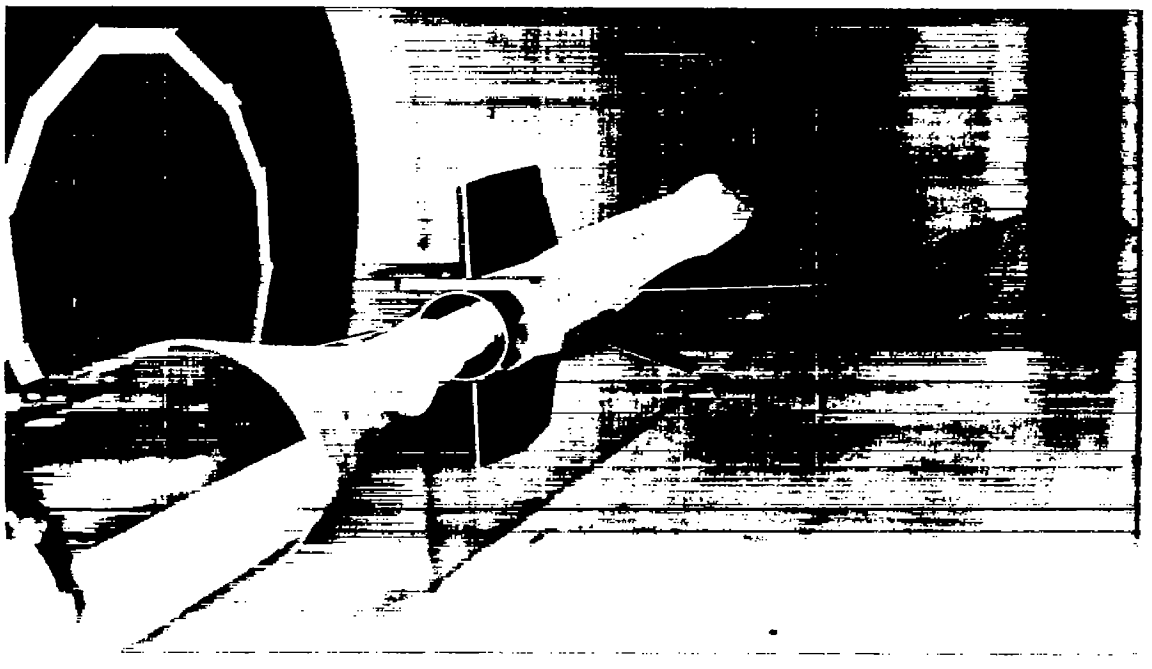

A-22163

(b) Rear-quarter view.

Figure 3.- Photographs of the model in the 8- by 7-foot test section of the Ames unitary plan wind tunnel.

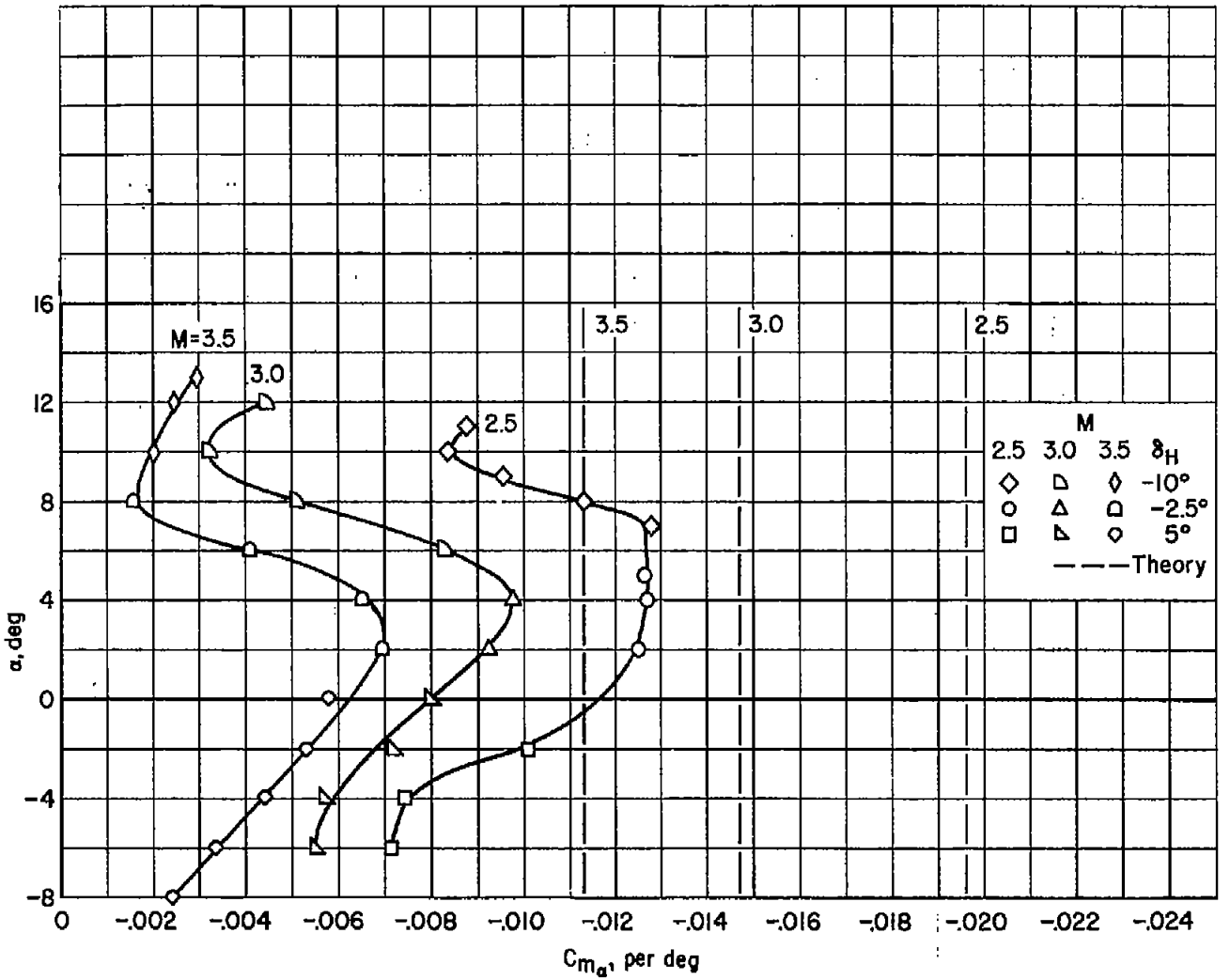

Figure 4.- The variation of the static longitudinal stability derivative with angle of attack for the basic configuration.

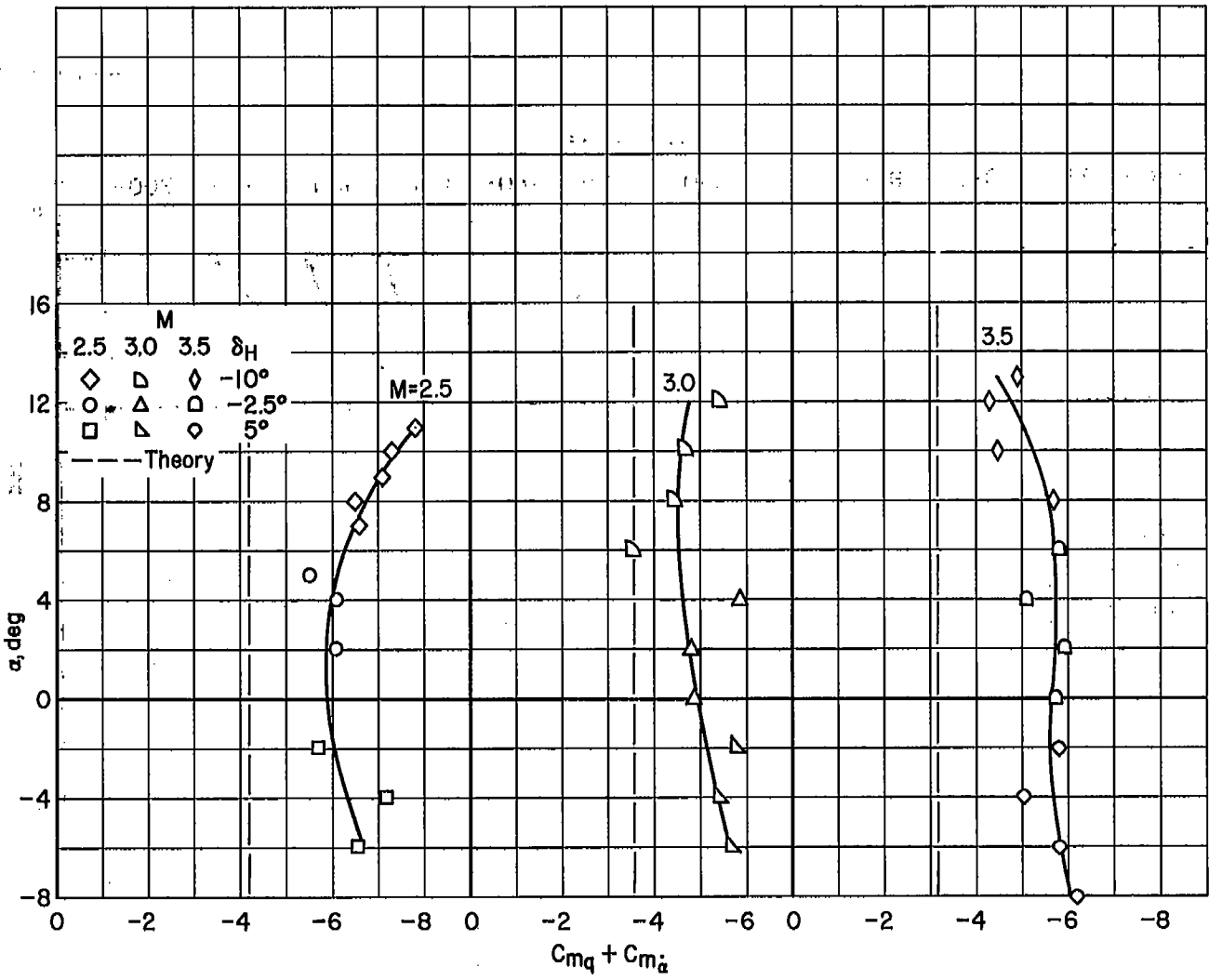

Figure 5.- The variation of the damping in pitch derivative with angle of attack for the basic configuration.

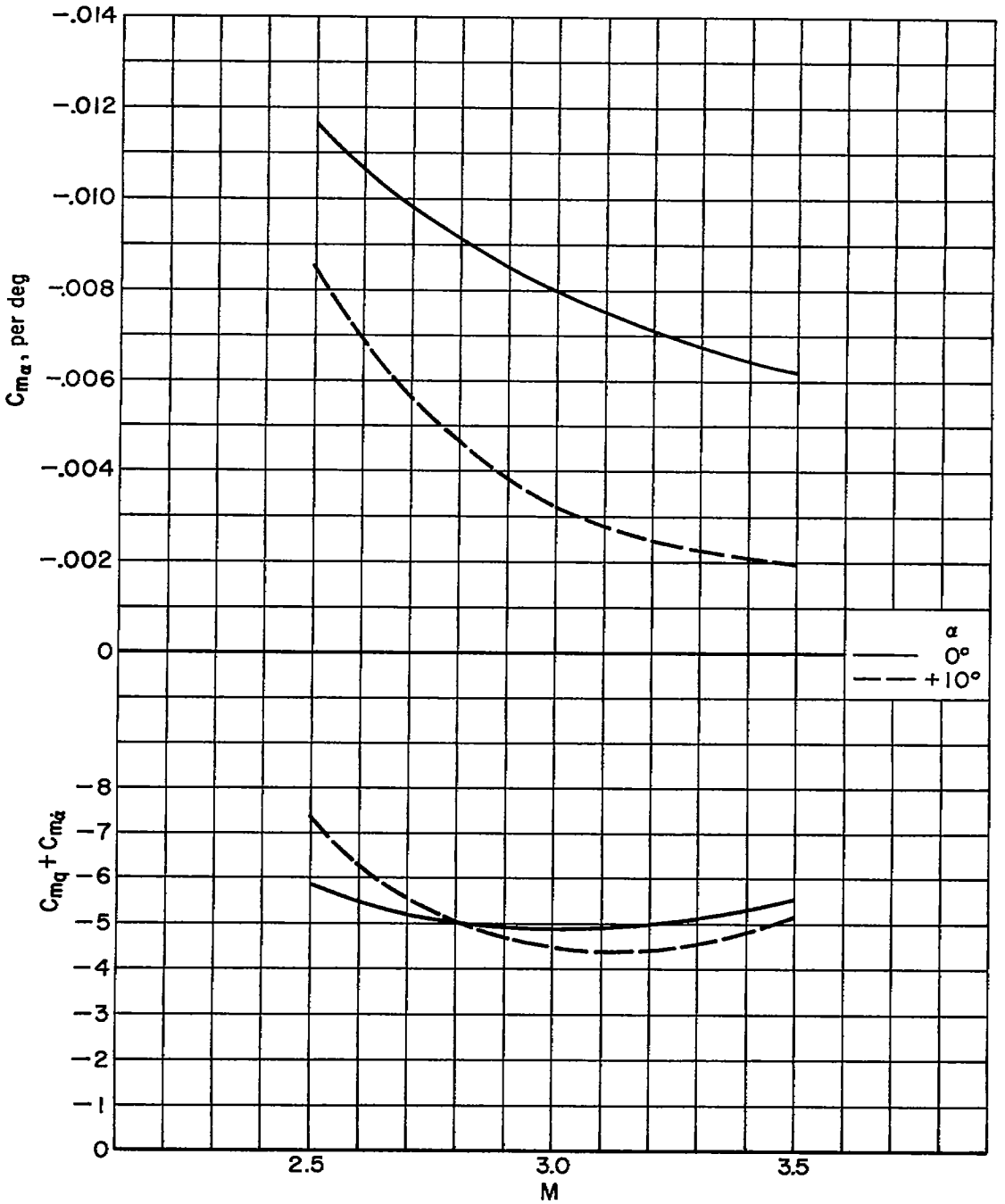

Figure 6.- The variation with Mach number of the static and dynamic longitudinal stability derivatives at two angles of attack for the basic configuration.

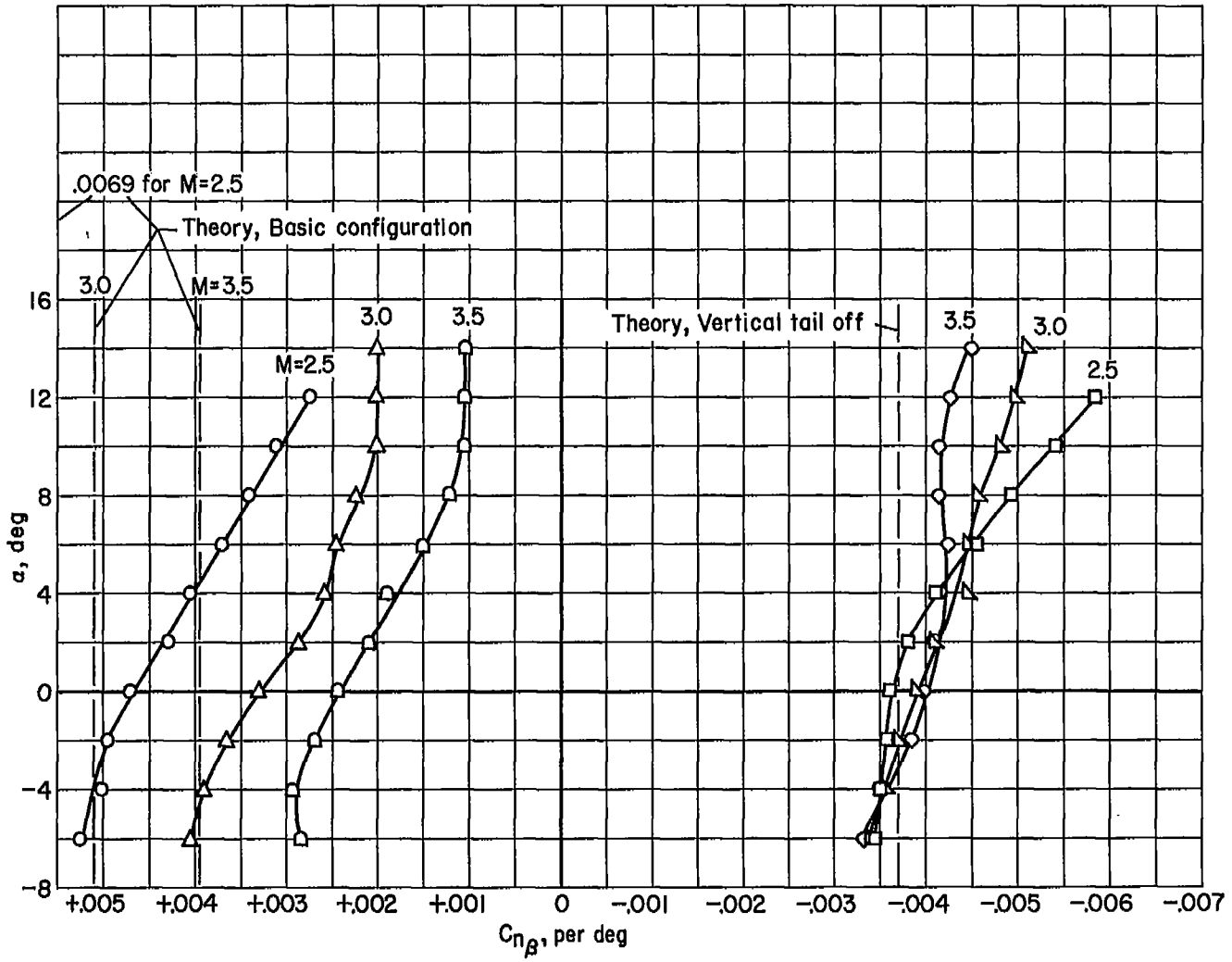

Figure 7.- The variation of the static directional stability derivative with angle of attack for the basic configuration and the configuration with the vertical tail removed; $\delta_H = -5^\circ$.

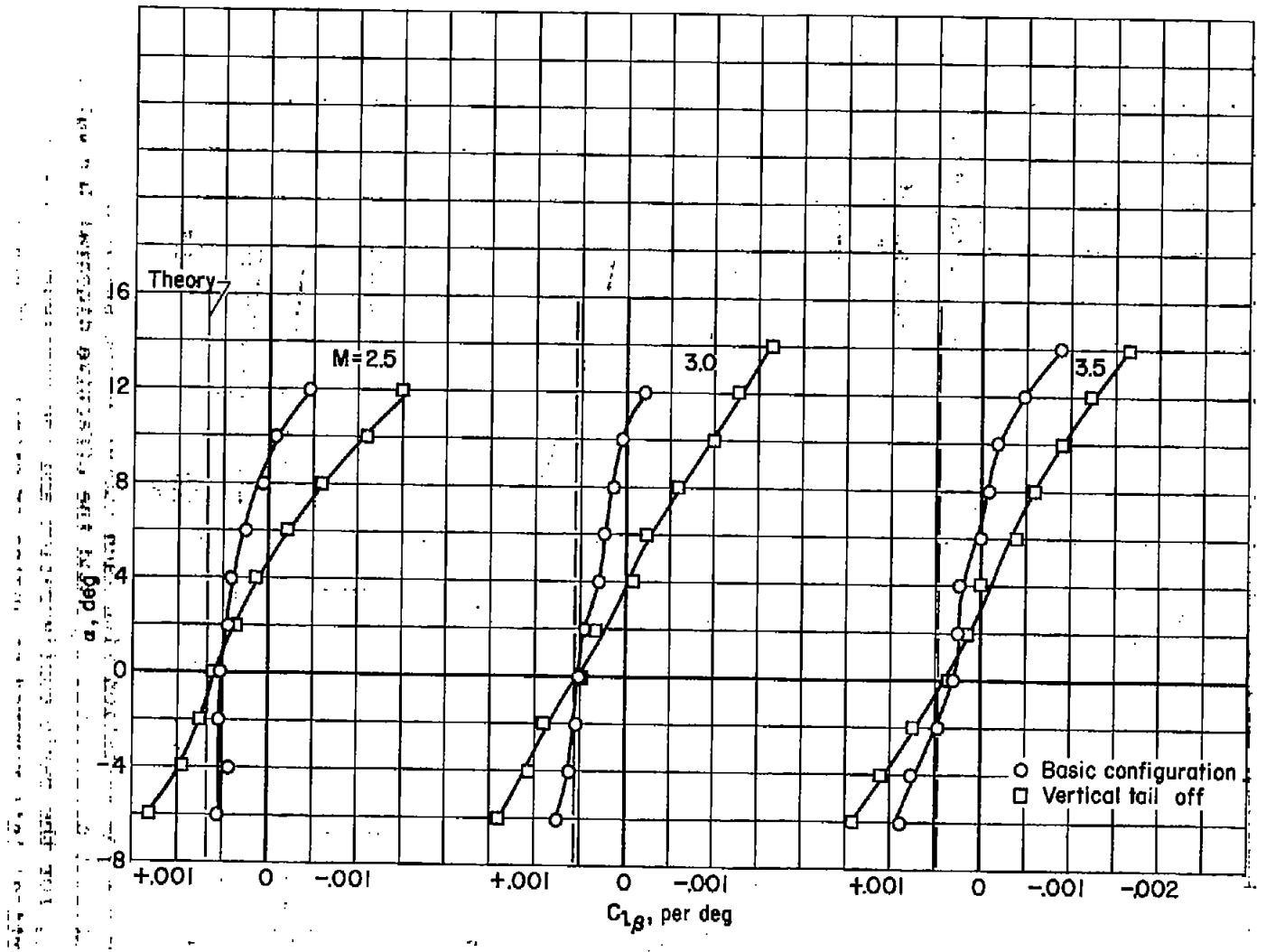

Figure 8.- The variation of the effective dihedral derivative with angle of attack for the basic configuration and the configuration with the vertical tail removed; $\delta_H = -5^\circ$.

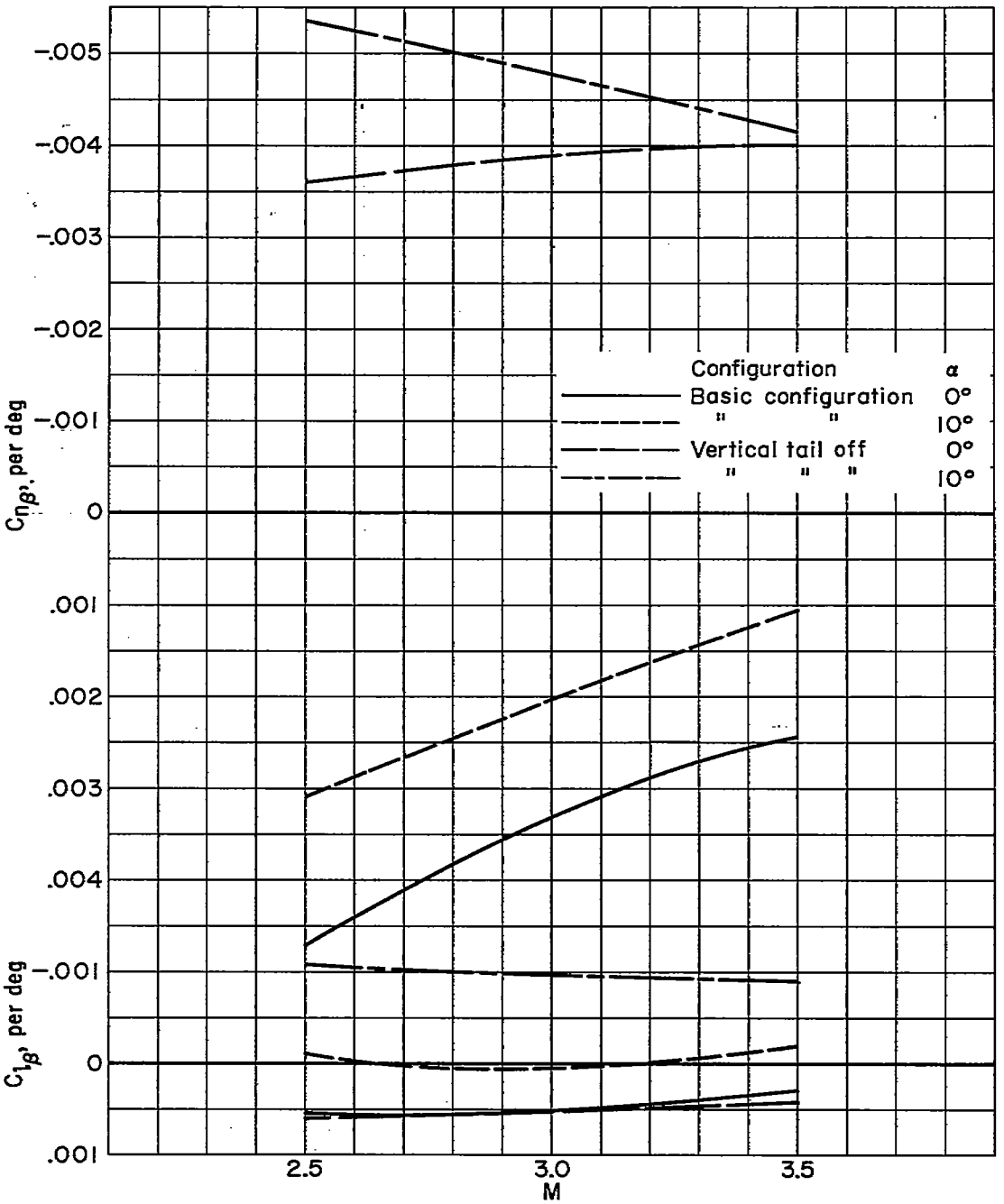

Figure 9.- The variation with Mach number of the static directional stability derivative, C_{n_β}, and the effective dihedral derivative, C_{l_β}, for the basic configuration and the configuration with the vertical tail removed at angles of attack of 0° and 10°; $\delta_H = -5°$.

[redacted]

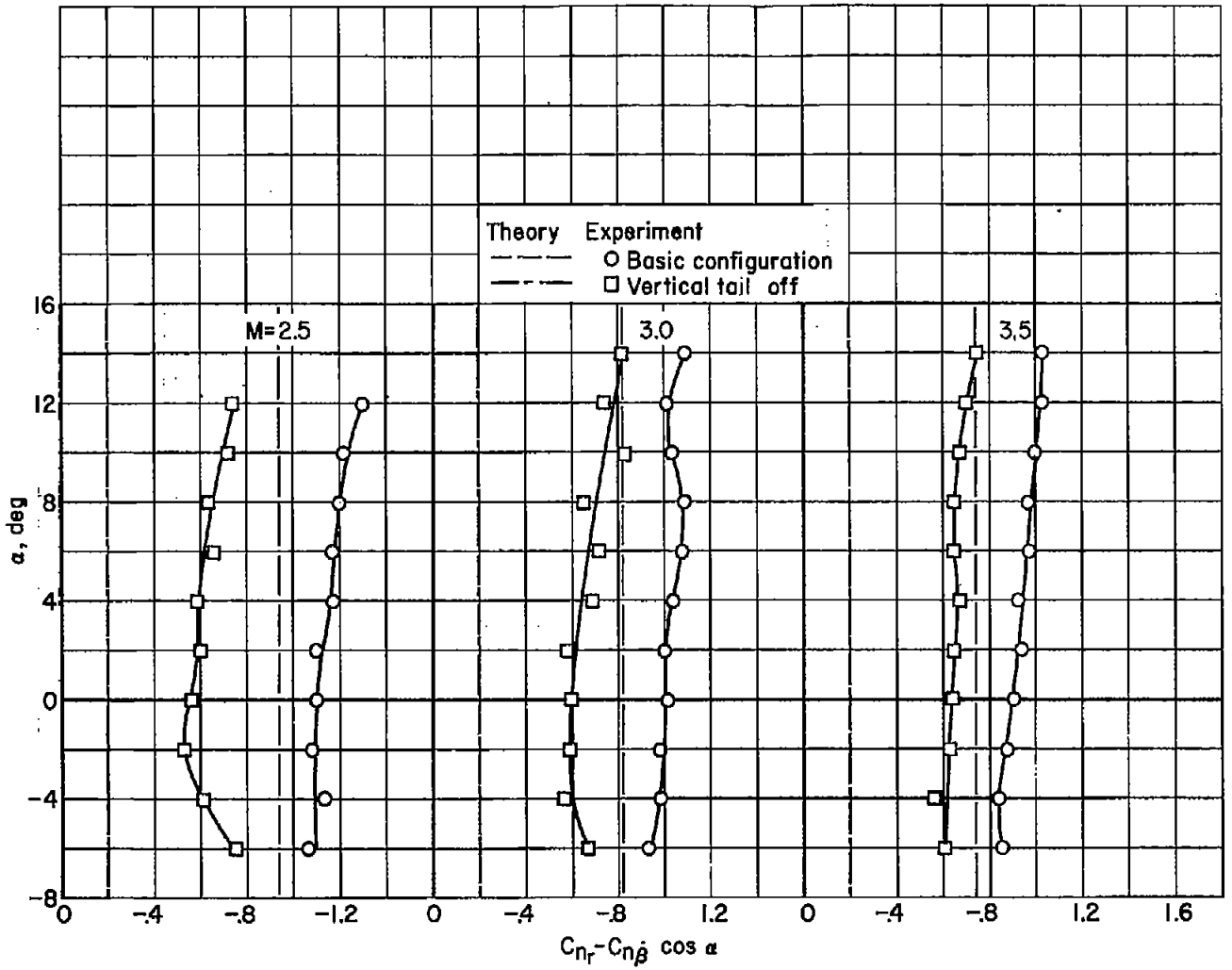

Figure 10.- The variation of the damping in yaw derivative for the basic configuration and the configuration with the vertical tail removed; $\delta_H = -5^\circ$.

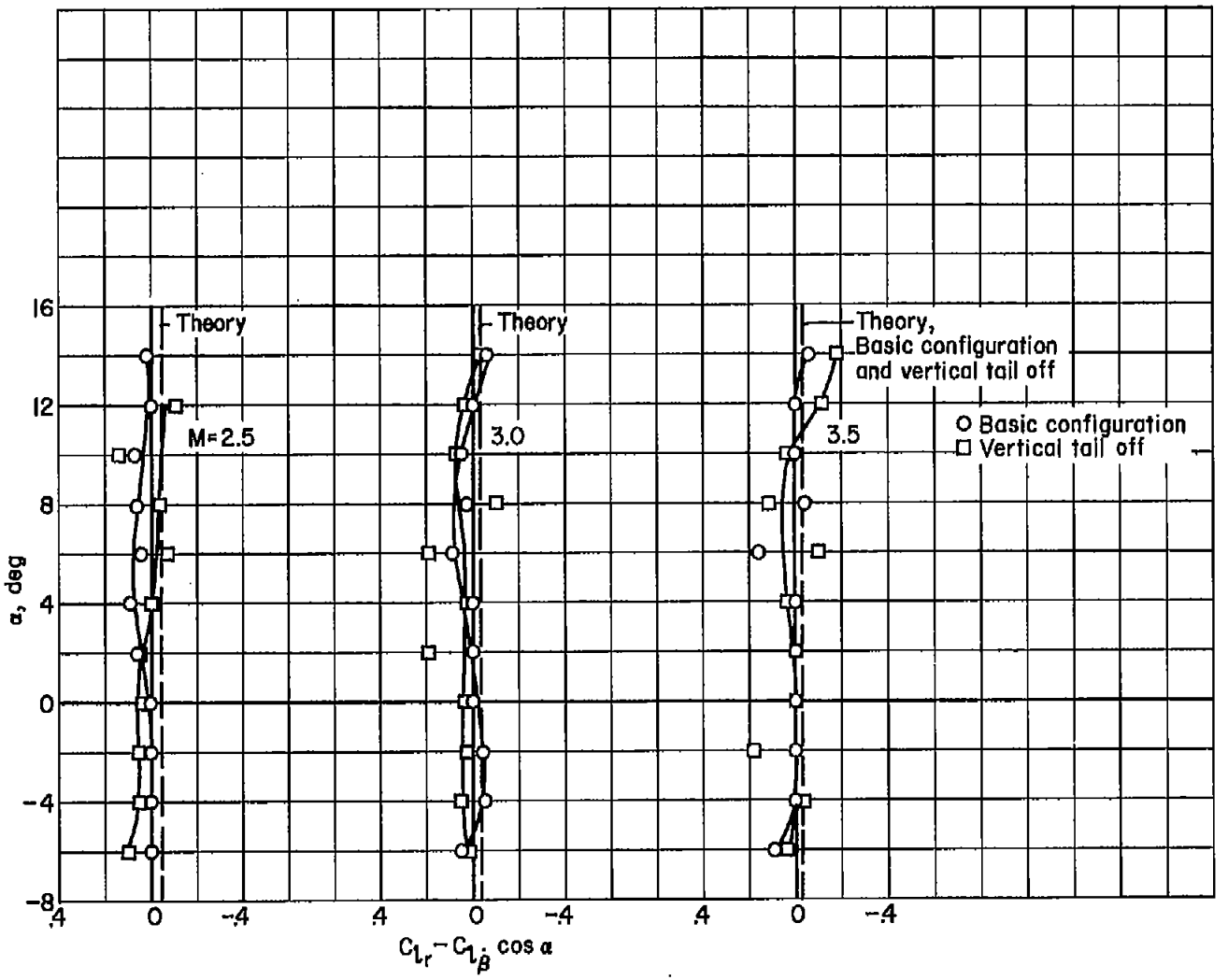

Figure 11.- The variation of the rolling moment due to yawing derivative with angle of attack for the basic configuration and the configuration with the vertical tail removed; $\delta_H = -5^\circ$.

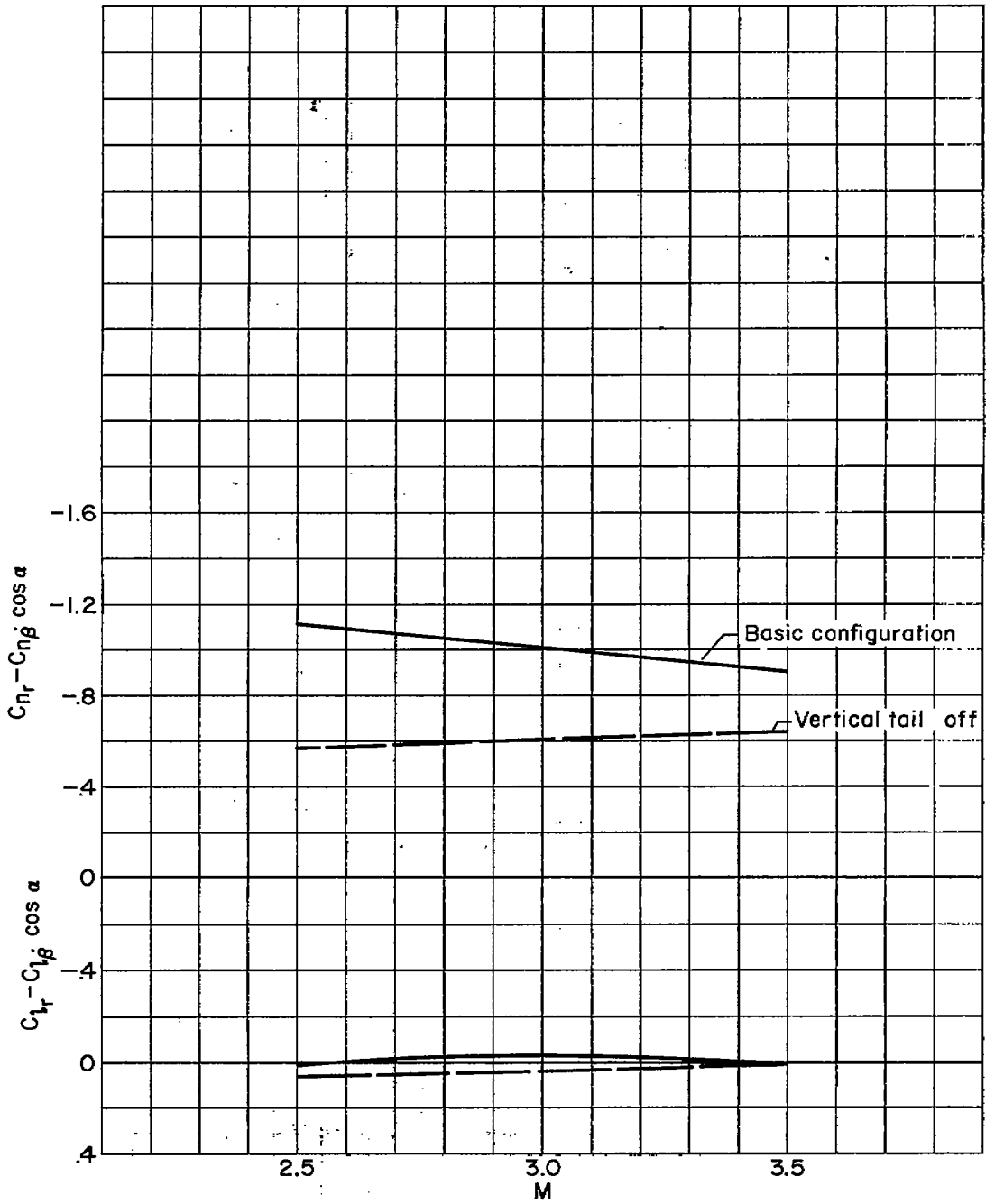

Figure 12.- The variation with Mach number of the damping in yaw derivative and the rolling moment due to yawing derivative for the basic configuration and the configuration with the vertical tail removed; $\delta_H = -5^\circ$.

[redacted]

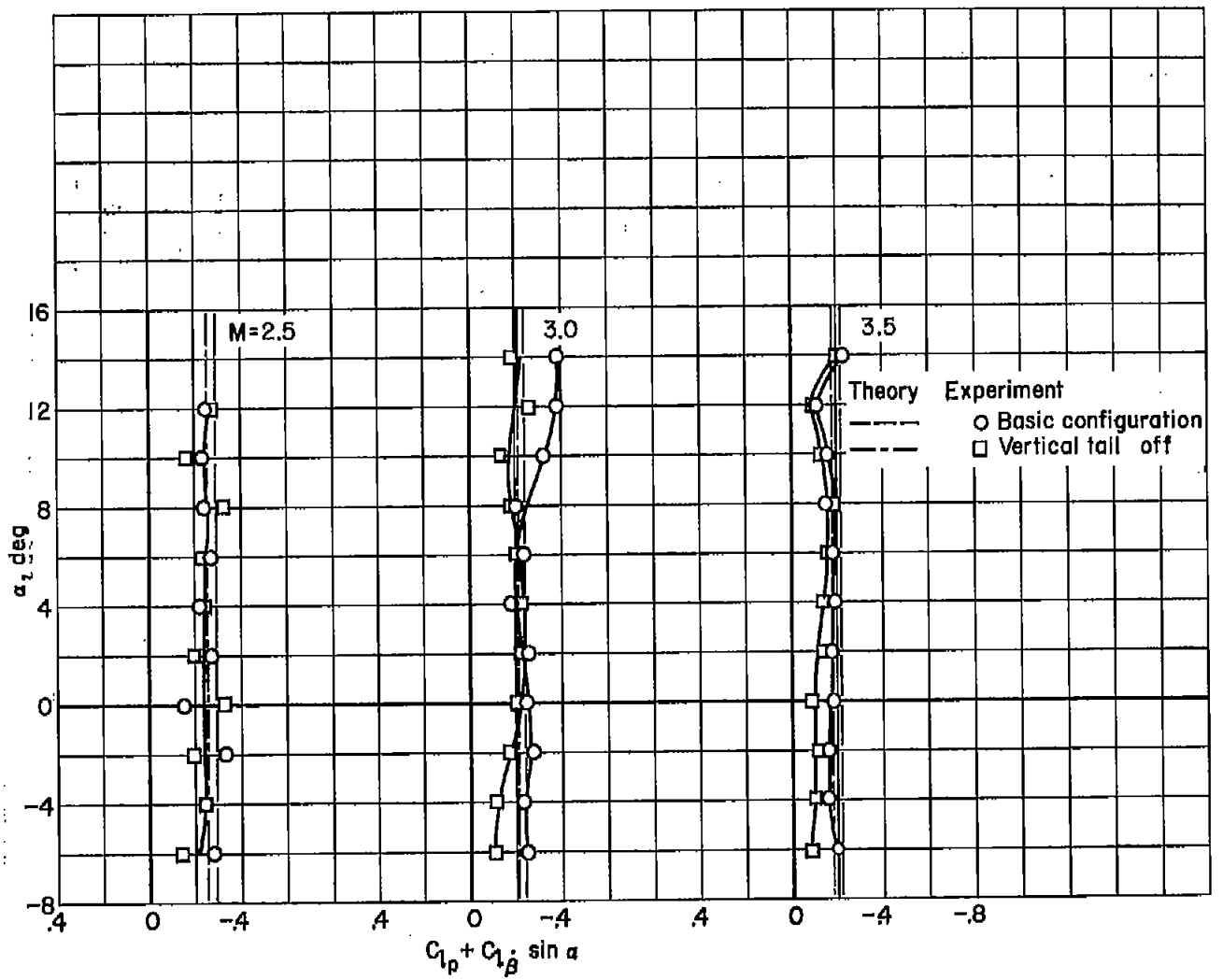

Figure 13.- The variation of the damping in roll derivative with angle of attack for the basic configuration and the configuration with the vertical tail removed; $\delta_H = -5^\circ$.

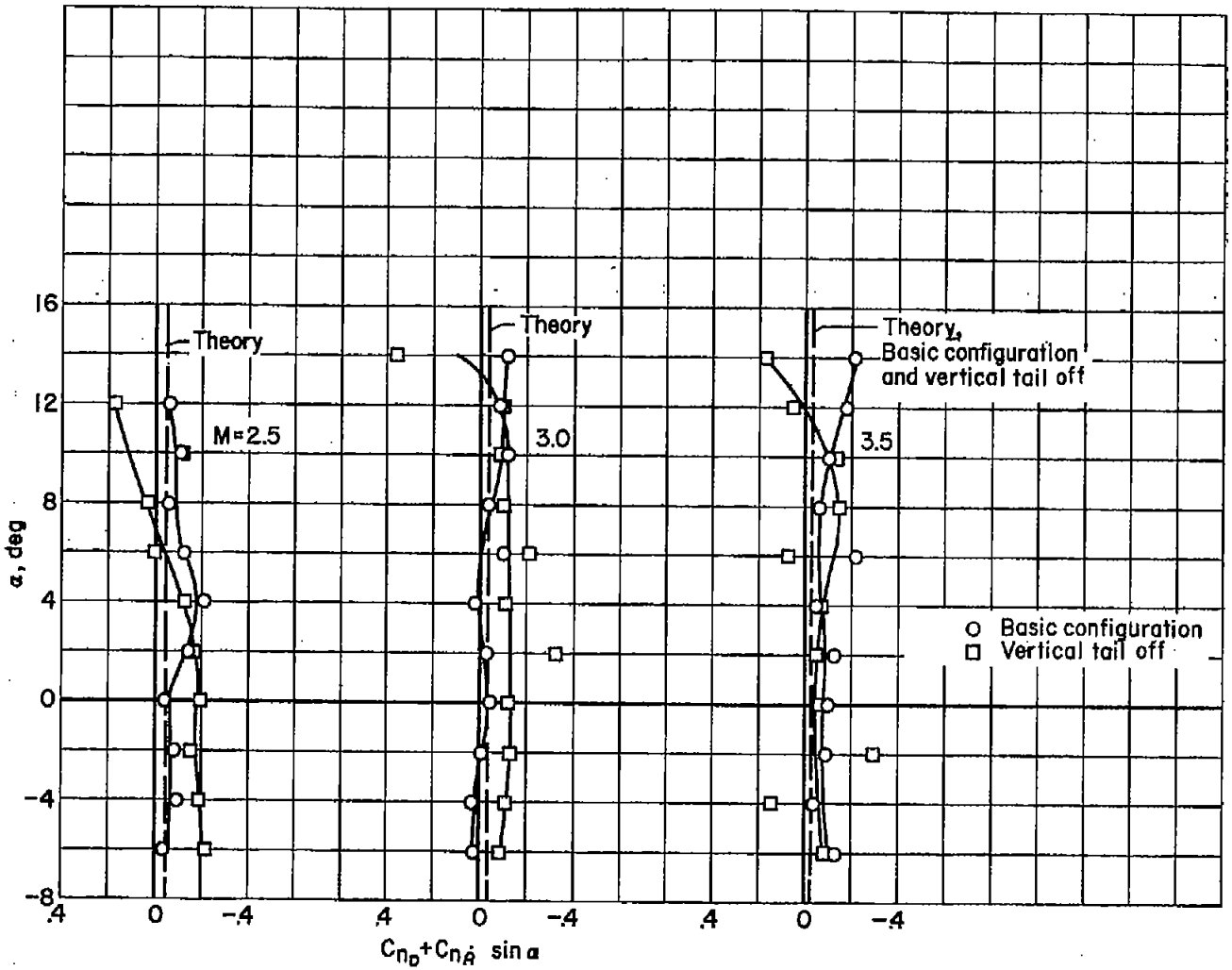

Figure 14.- The variation of the yawing moment due to rolling derivative with angle of attack for the basic configuration and the configuration with the vertical tail removed; $\delta_H = -5^\circ$.

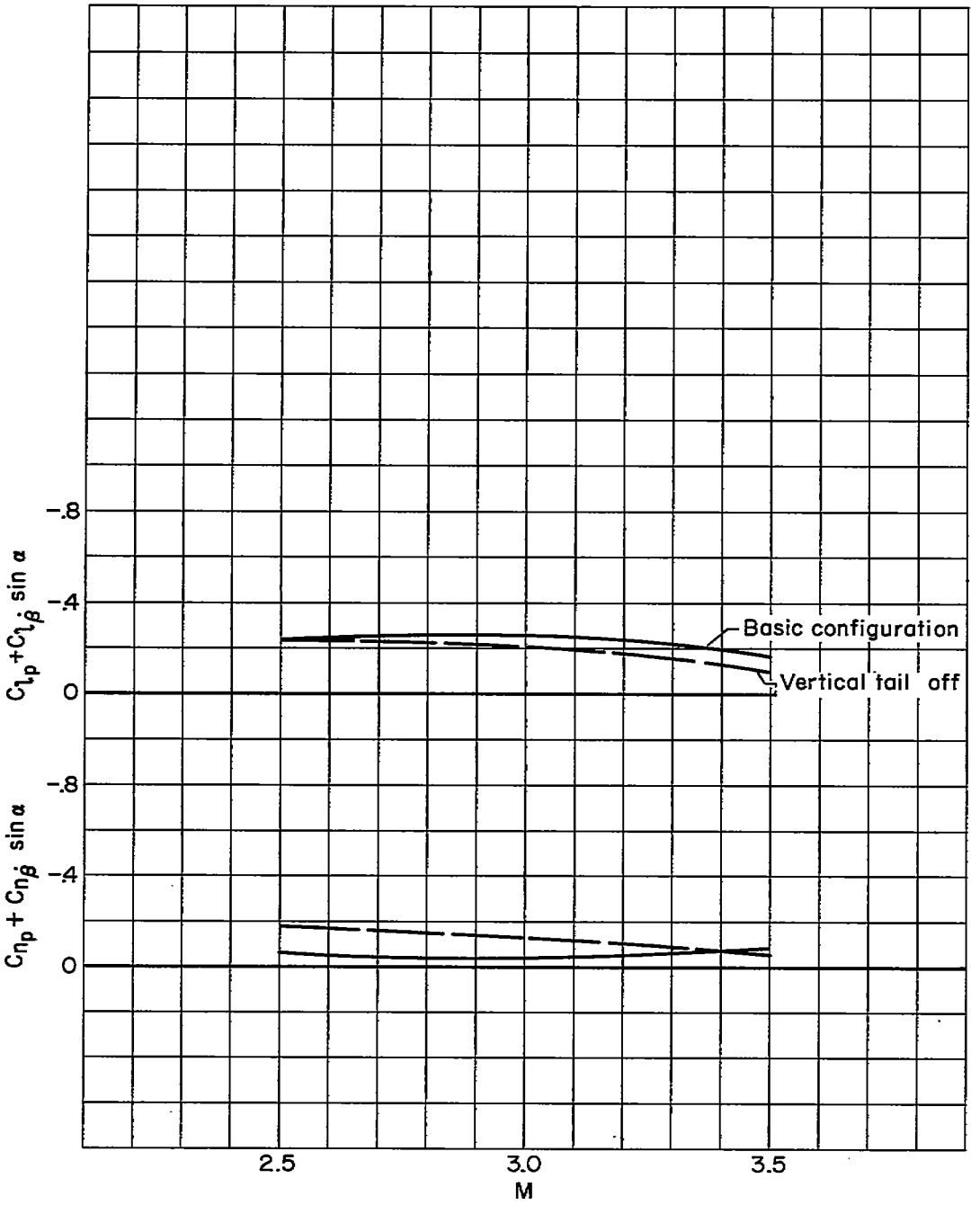

Figure 15.- The variation with Mach number of the damping in roll derivative and the yawing moment due to rolling derivative for the basic configuration and the configuration with the vertical tail removed; $\delta_H = -5^\circ$.

[redacted]